Biomacromolecules

Subscriber access provided by SEOUL NATIONAL UNIV OF TECH

Article

Effects of molar ratios of two immiscible monomers towards development of amphiphilic, highly stretchable, bioadhesive, self-healing copolymeric hydrogel and its mineral active cellular behavior

Dipankar Das, Eunchong Cha, Sangji Lee, HyunSoo Shin, and Insup Noh

Biomacromolecules, **Just Accepted Manuscript** • DOI: 10.1021/acs.biomac.9b01560 • Publication Date (Web): 02 Jan 2020

is published by the American Chemical Society. 1155 Sixteenth Street N.W., Washington, DC 20036

Effects of molar ratios of two immiscible monomers towards development of amphiphilic, highly stretchable, bioadhesive, self-healing copolymeric hydrogel and its mineral active cellular behavior

Dipankar Das,[a,b] Eunchong Cha,[b] Sangji Lee,[b] HyunSoo Shin,[b] Insup Noh[a,b*]

[a]Department of Chemical and Biomolecular Engineering, Seoul National University of Science and Technology, Seoul 01811 Korea (Republic of)

[b]Convergence Institute of Biomedical Engineering and Biomaterials, Seoul National University of Science and Technology, Seoul 01811 Korea (Republic of)

*Corresponding author: Email: insup@seoultech.ac.kr

Tel: +822-970-6603; Fax: 02-977-8317.

Submitted Revised version to *Biomacromolecules* (December 2019)

Abstract

Here, we report the striking properties such as high stretchability, self-healing, and adhesiveness of an amphiphilic copolymeric hydrogel (PAA-PMMA gel) synthesized from two immiscible monomers—acrylic acid (AA) and methyl methacrylate (MMA)—through a simple free radical polymerization in an aqueous medium. The developed hydrogel with a specific molar ratio of MMA and AA, is self-healable, which is attributed to the hydrophobic interaction arises from methyl groups of PMMA, as well as the breakdown and reformation of sacrificial noncovalent crosslinking through the weak hydrogen bonds between the carboxylic acid groups of PAA and methoxy groups of PMMA. The energy dissipation values in the hysteresis test signify the excellent self-recoverability of the hydrogel. The developed hydrogel showed adhesive behavior to the surfaces of polystyrene, glass, wood, metal, stone, ceramics, pork skin and human skin. The physical and mechanical properties of the PAA-PMMA gel were fine-tuned through changes in the MMA/AA ratio and pH. Moreover, the PAA-PMMA hydrogel can serve as a template for calcium phosphate mineralization to yield a hydrogel composite which improved MC3T3 cell adhesion and proliferation. Overall, we propose that depending on synthesis parameters and other scenarios, the synthesized PAA-PMMA hydrogel could potentially be employed in varying biomedical and industrial applications.

Keywords: Bioadhesive, hydrogel, physical crosslinking, self-healing, stretchable

1. Introduction

Over the past few years, novel hydrogel systems developed with functional characteristics (e.g., durability, high stretchability, adhesiveness, self-healing capacity) have received significant attention because their physicochemical properties can be fine-tuned and their flexibly deforming nature is attractive [1-6]. The features of these gels suggest they may have utility across a broad spectrum of applications like as superabsorbent materials [1, 2, 4], in waste-water treatment [7], electronics [8-11], sensors [12, 13], and biomedical fields [14-16]. Self-healing potential is a striking attribute capable of instinctively repairing physical damage, an event that is commonly observed in nature including in living organisms [17]. Self-healing materials could significantly advance the safety, durability, profit and ecological impact of synthetic materials [5, 9]. There are two types of self-healing mechanisms: i) extrinsic self-healability, a process which requires pre-storing healing reagents like monomers or catalysts inside microcapsules or microvascular networks [17-19], and ii) intrinsic self-healability, a capacity primarily mediated by dynamic covalent bonding (e.g., Diels–Alder reaction [20, 21], cycloaddition reaction [22], disulfide [23], radical dimerization reaction [24]) or reversible physical interactions (e.g., hydrogen bonding [3, 25, 26], host–guest interactions [10]). In reality, self-healing occurs when polymer chains can diffuse across a broken edge over time. Hence, the mobility of polymer chains is a fundamental factor for self-healability [17]. Higher chain mobility makes most existing self-healable polymers soft and flexible. Conversely, polymers employed in routine life and technical areas are generally strong and rigid; these polymers are associated with limited polymer chain mobility. Achieving and optimizing stiffness and self-healability simultaneously within a material is highly challenging, yet desirable for science and industry.

Among physical interactions, functional polymers with reversible hydrogen bonding have been extensively employed for the synthesis of comparatively tough hydrogels or healing

materials [3, 26]. For instance, Dankers *et al.* reported synthesis of self-healing polymers with mechanical properties controlled by molecular interactions of quadruple hydrogen-bonding, based on poly(ethylene glycol) and 2-ureido-4-pyrimidinone end-capped with four-fold hydrogen bonding units [27]. Jeon *et al.* described the development of a highly stretchable and self-healing hydrogel mediated through hydrophobic interactions [28]. Hu *et al.* prepared N, N'-dimethylacrylamide and methacrylic acid-based resilient hydrogels with shape-memory activities, where both weak hydrogen bonding association and hydrophobic interaction contributed to improved mechanical properties [25, 29]. Phadke *et al.* depicted self-healable hydrogels cross-linked by acryloyl-derivatized 6-aminocaproic acid and glycinamide based hydrogen bonding [30]. Recently, Teng *et al.* designed self-healable hydrogels with mineralization-active functions by leveraging weak hydrogen bonds and hydrophobic interactions initiated by oligo(ethylene glycol) methacrylate and methacrylic acid [3]. Inspired by a review of the relevant literature, we synthesized self-healing hydrogels by using commercially available, immiscible monomers such as methyl methacrylate (MMA) and acrylic acid (AA) *via* physical crosslink induced mechanism, even though reports of PMMA and PAA-based copolymers and hydrogels for different applications in different forms and with external cross-linkers or nanoparticles are available [6, 31-37]. For example, Halacheva *et al.* described pH-responsive biocompatible and biodegradable hollow particle gel scaffolds of poly(MMA-*co*-AA) cross-linked with either cystamine or 3,3′-dithiodipropionic acid dihydrazide for tissue regeneration [6]. An amphiphilic colloidal copolymer of MMA and sodium acrylate was developed through emulsion polymerization by Shih and colleagues [31]. A copolymerization reaction between AA and MMA in DMSO was reported by Ekpenyong *et al.*[37]. Additionally, polyaniline-poly(MMA-*co*-AA) films have been used as a corrosion inhibitor by Oliveira *et al.* [32] and Sayar *et al.* reported on the synthesis of a Fe_3O_4

nanoparticle-loaded poly(MMA-*co*-AA) composite [33]. Furthermore, Barba *et al.* outlined their approach to preparing poly(MMA-AA) copolymers for drug delivery applications [34] and Gyurova *et al.* described a pH-sensitive poly(MMA-*co*-AA) and investigated the effect of AA [35]. Yan *et al.* synthesized poly(AA-*co*-MMA) micro-particles for cisplatin delivery [36]. Despite all of this research, however, there are no reports on the design of a stretchable, self-healing, bioadhesive hydrogel using immiscible MMA and AA monomers in aqueous medium.

In this study, we report on a co-polymeric hydrogel decorated with physical crosslinking that leads to self-healing capacity, adhesiveness, and higher mechanical strength; this hydrogel was the product of aqueous free radical polymerization of MMA and AA, without using any external crosslinker. MMA was selected because it contains both methyl group (-CH_3) that can form hydrophobic interaction and the methoxy oxygen atom (-OCH_3) which can serve as hydrogen-bond acceptor, while AA is an effective hydrogen-bond donor. In the synthesized hydrogel network, MMA and AA were covalently bonded, and whereas, the weak hydrogen bonds (between –COOH of PAA and –OCH_3 of PMMA) act as sacrificial and reversible crosslinks which import remarkable physical properties to the copolymeric hydrogel. The hydrophobic interaction and weak hydrogen bonding interaction between MMA and AA are mainly responsible for the recoverability, and self-healing behaviour of the hydrogel, which is also reversible with pH and depends on monomers composition in a gel network. Furthermore, the existence of carboxylic acid groups in the hydrogel network can act as a template for calcium phosphate mineralization to improve biocompatibility such as cell adhesion and proliferation. It is believed that these first observable striking properties of PAA-PMMA hydrogel would be useful for a number of biomedical and industrial applications.

2. Materials and methods

2.1. Materials

Acrylic acid (AA, Sigma Aldrich, USA), methyl methacrylate (MAA, Sigma Aldrich, USA), potassium peroxodisulfte ($K_2S_2O_8$, Sigma Aldrich, Germany), potassium dihydrogen phosphate (KH_2PO_4, Sigma Aldrich, USA), disodium hydrogen phosphate (Na_2HPO_4, Sigma Aldrich, UK), calcium chloride ($CaCl_2$, Sigma Aldrich, Japan), dimethyl sulfoxide-D_6 (DMSO-D_6) and sodium hydroxide (NaOH, Yakuri pure chemicals Co. Ltd., Kyoto, Japan) were purchased and used for experiments. Double distilled water (DW) was employed for all studies.

2.2. Hydrogel synthesis:

The hydrogel was synthesized using an aqueous free radical polymerization technique. In brief, at first, 2 mL of double distilled water (DW) and a magnetic stir bar were kept in a 20 mL glass vial (**Figure 1a**). Afterwards, the required amount of MMA (**Table S1, Supporting Information**) was added in the DW (**Figure 1b**). After that, the requisite amount of AA (**Table S1, Supporting Information**) was added dropwise in the solution at room temperature and 120 rpm until the medium became clear (**Figure 1c-e**). Then, 0.003 g of potassium peroxodisulfte (KPS) was dissolved in the solution by bubbling nitrogen gas for 10 min. Next, the stir bar was removed and the glass vial was closed tightly with a cap and kept it in an oil bath at 75 °C for 7 h. Finally, after heating, the white-coloured gel samples (PAA-PMMA hydrogel) were taken out after reaching room temperature and used for other experiments. Three grades of PAA-PMMA hydrogels were prepared and the gels were designated as Gel 1, Gel 2 and Gel 3 (higher number indicates an increasing amount of MMA).

2.2.1. Mineralization of hydrogel:

The prepared gel samples were mineralized using an alternative soaking method after slight modifications as described in the literature [3]. Briefly, the gel samples were first immersed into a phosphate buffer solution (PBS, pH 7.4) overnight to attain an equilibrium swelling state. During this step, the pH was adjusted to pH 7.4 by adding NaOH solution. Next, hydrogels were soaked in 0.5 (M) $CaCl_2$ solution for 1 h and then washed with DW three times to remove excess calcium ions. Afterwards, the gel samples were immersed into 0.3 (M) K_2HPO_4 solution for 1 h and then washed with DW three times to remove excess reagent. Both processes were alternatively repeated three times to mineralize the hydrogels with calcium phosphate. After three cycles, the gel samples were immersed into PBS (pH 7.4) for 3h, washed with DW and used for experiments. The mineralized gels were named Gel 1-M, Gel 2-M, and Gel 3-M.

2.3. Characterization:

Fourier-transform infrared (FTIR) spectra of MMA, AA, and dried gel samples were recorded using an FTIR Spectrometer (Model: Cary 630, Agilent Technologies, USA) in attenuated total reflectance (ATR) mode. ^{1}H-Nuclear magnetic resonance (NMR) spectra were detected with a 700 MHz nuclear magnetic resonance (NMR) spectrometer (Model: DD2 700, Agilent Technologies, USA) in DMSO-d_6 solvent. Thermogravimetric analysis (TGA) was performed at KOPTRI (Seoul, Korea) using a thermogravimetric analyser (Model: TGA Q500, USA) in nitrogen atmosphere, where the temperature range was 30-700 °C and heating rate 5 °C/min. Differential scanning calorimetry (DSC) analysis was done using a differential scanning calorimeter (Model: DSC-60, Shimadzu, Japan), in nitrogen atmosphere, where the temperature range was 25-350 °C and heating rate was 10 °C/min.

The surface morphology of lyophilized gels and internal morphology of the mineralized gels were examined by scanning electron microscope (SEM; Model: TESCAN VEGA3, Czech Republic). Mineralized gel morphologies were examined by high resolution field emission scanning electron microscope (HR-FESEM; Model: SU8010, Hitachi High Tech. Co., Japan). Calcium content in the gel samples was identified using energy-dispersive X-ray spectroscopy (EDX). Mechanical properties of the gel samples were measured using Stable Micro Systems (Model: TA.XT plus texture analyser, Surrey, UK), by employing the maximum load of 50 N. The compression tests of the cylindrical gel samples (diameter = 24 mm, height = 5 ± 1 mm) were done in distance mode with a test speed of 1 mm/min. The tensile test was conducted at a test speed of 100 mm/min. Strain variation tests were performed in bottom mode at 20 N force and 1 mm/min speed at 25 °C. All tests were done twice and average values are reported.

2.4. Self-healing test:

The self-healing ability of native gel samples as well as self-healed gels was determined using tensile experiments as described below. The gel samples (length= 24 mm, width = 13 mm, height = 5 ± 1 mm) were cut into two pieces and then the cut portions were attached by slight handling pressure (less than 1 min) and kept in a Teflon box for 1 h and 12 h at 25 °C. After that, the tensile tests of the self-healed samples were performed with texture analyser at a pulling rate of 100 mm/min and 25 °C. All tests were done twice and average values are reported. The effect of pH on self-healing behaviour was achieved using the cylindrical-shaped hydrogel (Gel 2). First, the Gel 2 pieces were immersed in an HCl solution (pH 4.5) for 10 min, rinsed with distilled water, and then joined together by slight handling pressure. Similarly, the cut pieces were put in NaOH solution (pH 12) for 10 min. The separated hydrogels were then briefly rinsed with distilled water and then joined together by slight

handling pressure. To detect their reversible behaviour, after NaOH treatment and observation, the samples were put into pH 4.5 and then joined together by slight handling pressure.

2.5. Adhesion test:

The adhesive force of the gel samples towards varying object surfaces (i.e., ceramic, stainless steel, glass, iron, polystyrene, stone, wood, pork skin) was determined by texture analyser at a load of 5.0 g (0.05 N) and a test speed of 1.0 mm/sec. The return distance and contact time were 10 mm and 10 sec, respectively. All tests were done twice and average values are reported.

2.6. *In vitro* cell study:

The effect of the prepared gel on the *in vitro* growth and proliferation of osteoblast cells (MC3T3) was observed by covering cells with native gel (Gel 2) and mineralized gel (Gel 2-M) after they were seeded on a polystyrene culture dish. Cellular behaviours were assessed using a cell counting kit-8 (CCK-8) and the Live/Dead assay. The *in vitro* cytotoxicity assays of the swelled Gel 2 (at pH 7.4) and mineralized gel were performed using sample extracts as described in our previous reports [38, 39]. The MTT assay was used to calculate cell viability, where Teflon and latex were employed as positive and negative controls, respectively. The cell viability value of Teflon-treated cells was considered 100%. Statistical analysis was performed by one-way ANOVA using Tukey means comparison with Origin 8.0 software. The significance level was 0.05. Detail of cell study is given in the Supporting Information.

2.7. pH-responsiveness of gel:

The pH-responsiveness of the prepared gel samples was quantified using a swelling study

with acidic (pH 4.5) and basic buffer (pH 7.4) solutions. In brief, the lyophilized gel samples were immersed into buffer solutions in beakers for 24 h at 37 °C. At a regular time interval (1 h), gel samples were removed from the solutions and weighed after removing surface water with paper tissues. The % swelling ratio (SR) was calculated using the following equation [38, 40]:

$$Swelling\ ratio\ (\%) = \frac{W_t - W_d}{W_d} \times 100 \quad (1)$$

Where, W_t, W_d are weights of the swelled gels after the different time intervals, and the dried gels at the initial time, respectively. Each test was conducted in triplicate and the results are presents as Avg. ± S.D.

3. Results and discussion

3.1. Synthesis of hydrogel

The hydrogel was synthesized *via* a free radical polymerization technique using KPS as the initiator at 75 °C. Three different amounts of MMA (0.28 $\times 10^{-2}$ mol, 0.37 $\times 10^{-2}$ mol, and 0.47 $\times 10^{-2}$ mol) were used for gel synthesis. An interesting phenomenon occurred as AA was added to the MMA media, namely that the clear solution became turbid and phase separated before returning to a clear solution with the progressive addition of AA (**Figure 1a-e**). Specifically, when the ratio of MMA and AA reached 1:3.44 (for 0.47 $\times 10^{-2}$ mol MAA), 1:3.86 (for 0.37 $\times 10^{-2}$ mol MAA), and 1:4.50 (for 0.28 $\times 10^{-2}$ mol MAA), the solutions became clear (**Figure 1d-e**). When MMA was added to water, it was floated due to its hydrophobic nature. Due to the hydrophilic nature of AA, it was first miscible with water through intermolecular hydrogen-bonding interactions, which resulted in prominent phase separation (hydrophilic and hydrophobic layers) in the medium. However, further addition of

AA favoured the formation of additional weak hydrogen bonds between the methoxy group (-OCH_3) of MMA and the hydroxyl group (-OH) of the carboxylic acid unit of AA. As a result, a clear homogeneous solution was formed. It can be suggested that, at the critical monomer concentrations highlighted above, AA behaves like a phase-transfer agent. It is expected that additional hydrogen-bonding could influence the physical and chemical properties of the hydrogel.

In the presence of heat, KPS dissociates into sulphate anion radicals which may further react with water and create hydroxyl radicals (**Figure 1A**). It is assumed that these radicals attacked the double bond of either AA or MMA and initiated polymerization reactions between AA and MMA, thus forming co-polymeric hydrogels.

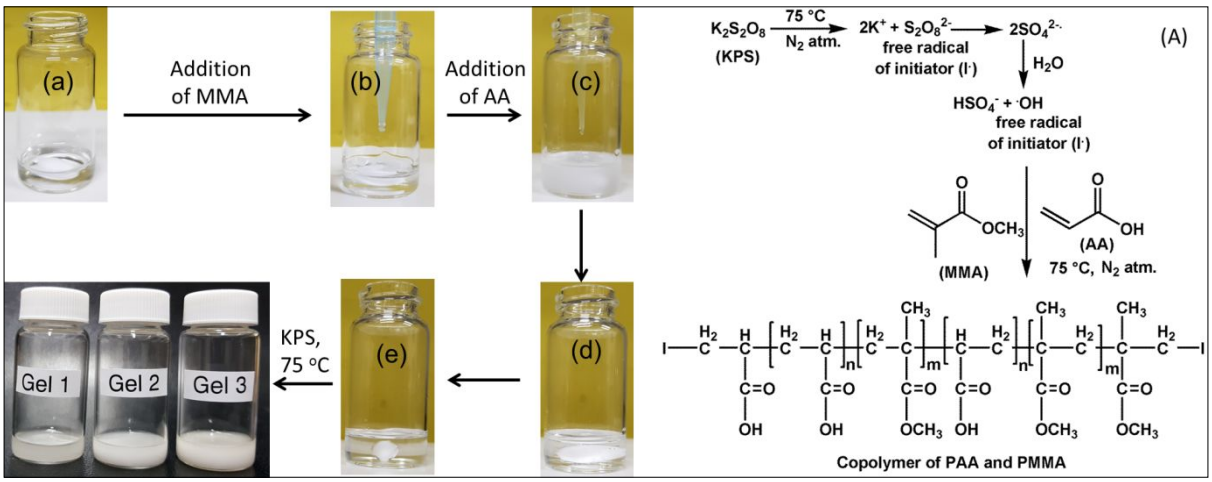

Figure 1. (a-e) Digital images of changing of reaction medium during the addition of MMA/AA, and PAA-PMMA hydrogel, and (A) probable reaction mechanism of hydrogel formation.

3.2. Characterization

The FTIR spectra of MMA, AA, and three gel samples are presented in **Figure 2**. In the FTIR spectrum of AA, the peaks at 3038, 2879, 1692, 1634, 1236 cm^{-1} indicate O-H, C-H, C=O,

C=C, C-O stretching frequencies, respectively. The peaks at 1429, 974 cm^{-1} are due to bending vibrations of C-O-H and O-H bonds. In the FTIR spectrum of MMA, the peaks at 2953 - 2929, 1718, 1636, 1196 - 1155 cm^{-1} are caused by C-H, C=O, C=C, and C-O-C stretching frequencies, respectively. As revealed in the FTIR spectra of the three gels, the absence of peak for C=C between 1634-1636 cm^{-1} signifies the formation of the MMA-AA copolymer through free radical polymerization. Interestingly, the shifting of C-O-H stretching vibration of the AA subunit (1429 cm^{-1} to 1409 cm^{-1}), and absence of peak representing O-H bonds bending, indicate that O-H bonds are connected by hydrogen bonds. Furthermore, the shifting of C-O-C stretching vibrations (1196-1155 cm^{-1} to 1161-1120 cm^{-1}) confirms the presence of hydrogen bonding between $–OCH_3$ groups (MMA) and -OH groups of –COOH (AA) (**Figure 2**).

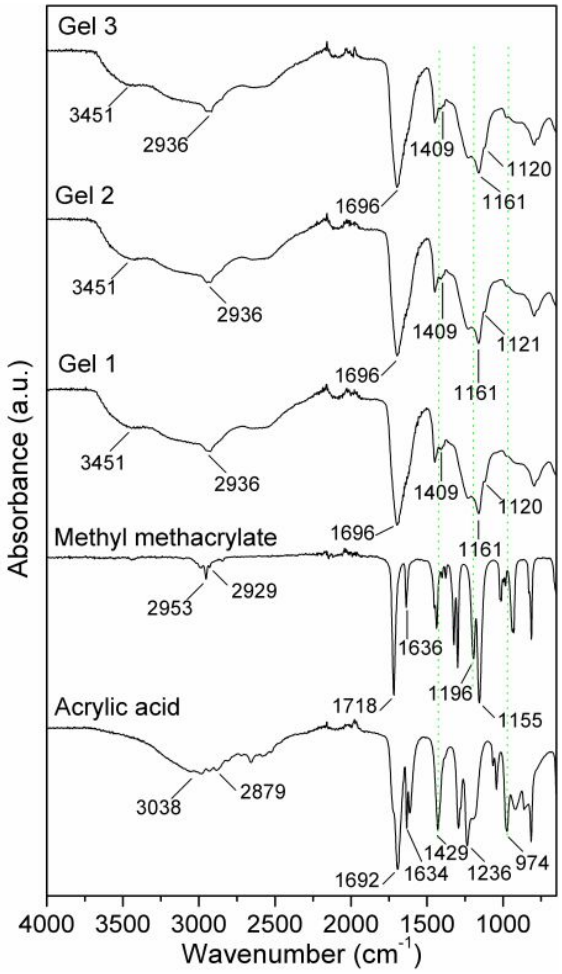

Figure 2. ATR-FTIR spectra of AA, MMA, and three dried PAA-PMMA gels

In the ^{1}H NMR spectrum of AA (**Figure 3**), the chemical shifts between δ = 5.84-6.25, δ = 12.43 ppm are owing to the presence of protons associated with double-bonded carbons (Ha-Hc), and carboxylic acid group, respectively. In the ^{1}H NMR spectrum of MMA (**Figure 3**), the chemical shifts between δ = 5.66-6.02, δ = 3.68, and 1.88 ppm are due to protons of double-bonded carbon (Ha, Hb), methoxy group (Hd) and methyl group (Hd), respectively.

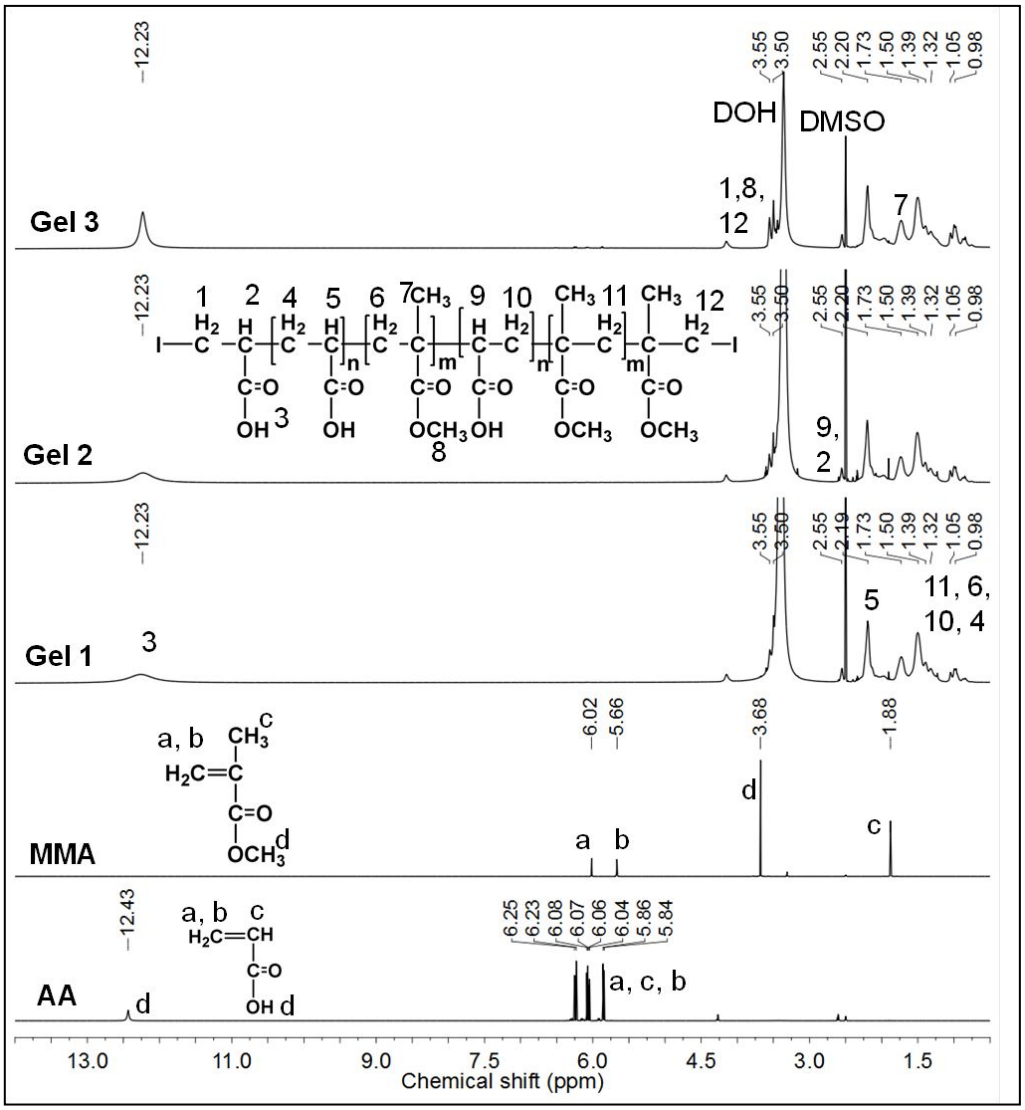

Figure 3. ^{1}H NMR spectra of AA, MMA, and three PAA-PMMA gels in DMSO-D_6 solvent

In the NMR spectra of the three gels (**Figure 3**), the chemical shift at δ = 12.23 ppm reflects the carboxylic acid group proton (H3), indicating the presence of an AA moiety. The chemical shifts for methoxy group protons (H8, δ = 3.50-3.56 ppm), and characteristics methyl group (H7, δ = 1.73 ppm) imply the existence of the MMA unit. Whereas, the absence of chemical shifts between δ = 5.66-6.25 ppm for protons of double-bonded carbons suggests polymerization of both MMA and AA moieties. The appearance of new chemical shifts for H1 – H6 and H9 – H12 protons between δ = 0.98-1.50, 2.55, 3.50-3.56 ppm established the

formation of the PAA-PMMA copolymer through free radical polymerization mechanism.

DSC study results revealed that the Tg and Tm of the co-polymeric gel appeared between 129.6-140.5 °C and 253.1-258.4 °C, respectively (**Figure S1a-c, Supporting Information**). The single Tg value clearly signifies that the PMMA and PAA units are thermodynamically miscible and exist as a homogeneous phase in the copolymeric network [31]. However, a non-monotonous trend of Tg values between Gel 1, 2 and 3 (129.6, 140.5 and 130.4 °C) could be attributed to the different degrees of hydrophobic and hydrogen bonding interactions. After a certain composition of MMA/AA, the hydrophobic repulsion between methyl groups alters the flexibility of the crosslinked network, which attributes to the lower Tg value of Gel 3 < Gel 2. In the TG and DTG plots (**Figure S1d-f, Supporting Information**), three major weight loss zones were observed. The first weight loss zone (between 268-310°C) implies decarboxylation from the PAA component [31]. The second weight loss region (between 320-390°C) is due to the decomposition of the PMMA unit, while the last one (between 400-460°C) signifies the complete disruption of PAA chains. These results indicate the higher thermal stability of PMMA and PAA segments in the copolymeric network rather than existence as a homopolymer.

SEM images of the dried gels (**Figure 4a-c**) reveal that gels contain microporous morphology. HR-FESEM images of the mineralized gels (**Figure 4d-f**) clearly reveal that various spherical calcium phosphate particles are produced after mineralization. It can also be observed that the surface roughness of gel samples is drastically increased after mineralization. SEM images of the internal morphology of the mineralized gels (**Figure 4g-i**) reveal the presence of calcium phosphate in the gel network. The EDX analysis results showed that Gel 1-M contains 35.40 % carbon, 50.17% oxygen and 6.91 % calcium atoms, respectively (**Figure S2-4 and Table S2-4, Supporting Information**). Whereas Gel 2-M

possesses 43 % carbon, 51.61 % oxygen and 3.47 % calcium atoms, Gel 3-M contains 38.75 % carbon, 51.50 % oxygen and 4.96 % calcium atoms (**Figure S2-4 and Table S2-4, Supporting Information**). The presence of calcium in the EDX analysis confirmed the mineralization of the synthesized gels. While, the average weight percentages (% w/w) of mineral particles of Gel 1, Gel 2, and Gel 3 are 0.97, 7.84, and 3.27, respectively.

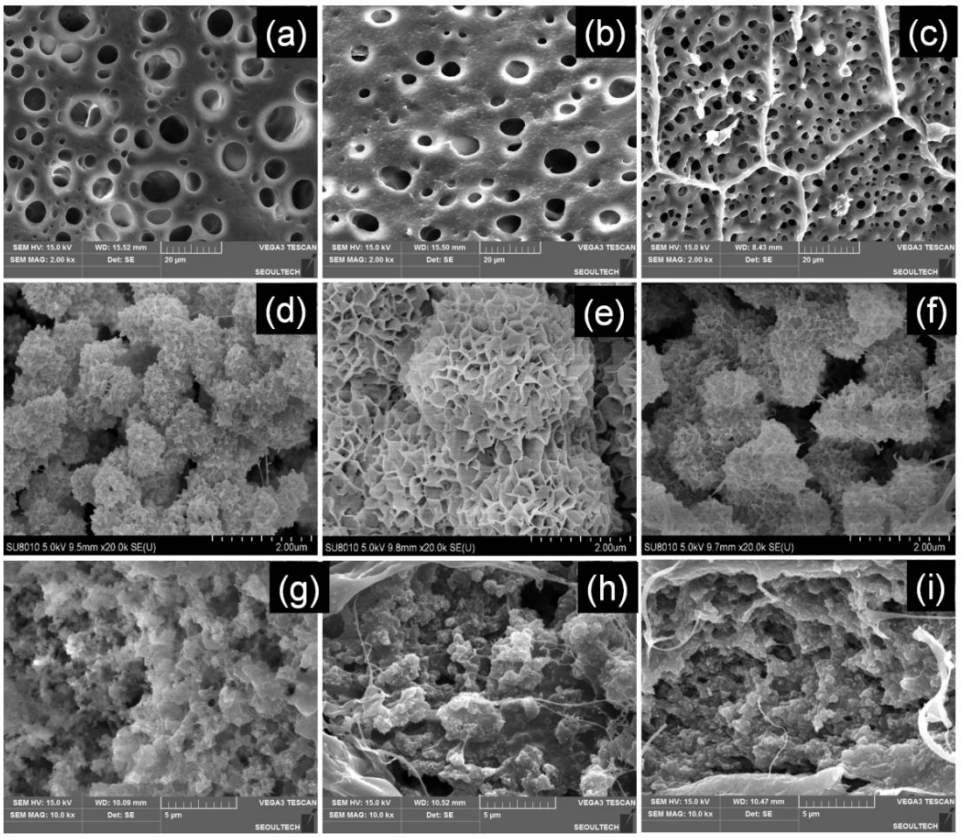

Figure 4. SEM images of: lyophilized Gel 1-3 (a-c), HR-FESEM mineralized Gel 1-3 (d-e), and cross-section of mineralized Gel 1-3 (g-i).

3.3. Self-healing and tensile test results

The self-healing nature of the prepared gels was assessed by both physical observation (**Figure 5A-P**), and tensile experimentation (**Figure 5a** and **Figure S5, Supporting Information**). Different shapes of samples were used to observe the healing nature of the

gels. **Figure 5A-D**, **Figure 5E-J**, and **Figure 5K-P** reveal the self-healing ability of Gel 1, Gel 2, and Gel 3, respectively. The samples were cut with a blade and then attached by handling pressure (for less than 1 min) and then left for 1 h and 12 h. One part of Gel 2 was coloured with aniline blue dye to easily distinguish between the two different parts of the gel (**Figure 5G-J**). Tensile experiment results (**Figure S5, Supporting Information**) of Gel 1 and Gel 2 reveal highly stretchable behaviours (up to 4266 ± 85 %). On the other hand, native Gel 3 was broken after ~3554 % extension, while the reattached Gel 3 was broken after ~1504 % extension (**Figure 5a**). These results demonstrate that the healing efficiencies [3] of Gel 1 and 2 were 100 % in the experimental conditions. However, the stress values of Gel 1 and Gel 2 decreased beyond the maximum stress with the increase of strain. This could be attributed to the formation of voids or small cracks in the hydrogels at the large strain before broken. On the other hand, Gel 3 showed ~42 % healing efficiency after 12 h. **Figure S6, Supporting Information** signifies that all three gels were broken and showed lower stretchability and healing efficiencies (~41 % for Gel 1, ~62 % for Gel 2 and ~7 % for Gel 3) while they reattached for 1 h compared to 12 h. The interesting healing characteristics could be attributed to (i) the rupture and reconstruction of reversible bonds (between the hydrogen atoms of carboxylic acid groups of PAA and oxygen atoms of methoxy groups of PMMA) which act as sacrificial crosslinking that facilitates the damaged area to self-heal[3], and (ii) the presence of hydrophobic interaction between methyl groups of PMMA in the gel network. While the lower healing efficiency of Gel 3 may be due to the existence of higher hydrophobic content that could generate a repulsive interaction which resists to complete reformation of the gel network. As can be seen in **Figure S7**, **Supporting Information,** physical interactions (eg, weak hydrogen-bonding and hydrophobic interactions between AA and MMA) may exist in the hydrogel matrix, which demonstrates natural self-healing

property at room temperature, exclusive of any additional healing substrates or external stimuli. In the hydrogel matrix, the weak hydrogen-bonding interaction (between the hydrogen atoms of carboxylic acid groups of PAA and oxygen atoms of methoxy groups of PMMA) acts as a physical cross-linker which generates intermolecular interactions between PMMA and PAA chains, resulting in the formation of the flexible three-dimensional cross-linked network. In the presence of tension or force, these weak hydrogen bonds could be re-established leading to self-healing capacity. When two cut pieces are exposed to one another through attachment, the dangling hydrogen bonds of the newly cut side recover co-facial interactive ends over time. A similar observation has been reported in the literature[3], and the hydrogen-bonding interactions are confirmed in this study by FTIR analysis. Shifting of the C-O-H stretching vibration (1429 cm^{-1} to 1409 cm^{-1}) of the AA unit, and absence of peaks for O-H bond bending, indicate that O-H bonds are connected by hydrogen bonds. Furthermore, shifting of the C-O-C stretching vibrations (1196-1155 cm^{-1} to 1161-1121 cm^{-1}) confirmed the hydrogen bonding between the $–OCH_3$ groups of MMA units and -OH groups of –COOH of AA units in the hydrogel network (**Figure 2**).

Furthermore, hydrogen bonds are also impacted by the thermal characterization of the hydrogel. In TGA analysis, the increased thermal stability of PMMA and PAA segments in the copolymeric network, rather than their existence as individual units (ie, in homopolymer form) suggest a strong interaction between the two subunits [31]. Besides, the single Tg value in the DSC strongly signifies that PMMA and PAA units are both thermodynamically miscible and exist as a homogeneous phase through both covalent and physical interactions in the co-polymeric network [31]. As shown in **Figure S7**, **Supporting Information** hydrogel characteristics are impacted by not only hydrogen bonds between -COOH and $–OCH_3$, but also intermolecular hydrophobic interaction between $–CH_3$ groups of PMMA units. Teng *et*

al. observed that the presence of $-CH_3$ groups on the polymer backbone enhanced hydrophobicity which promoted the rebuilding of the physical network [31]. Hence, it can be said that the excellent mechanical characteristics of the hydrogel are attributed to the formation of both hydrogen bonding and hydrophobic interaction.

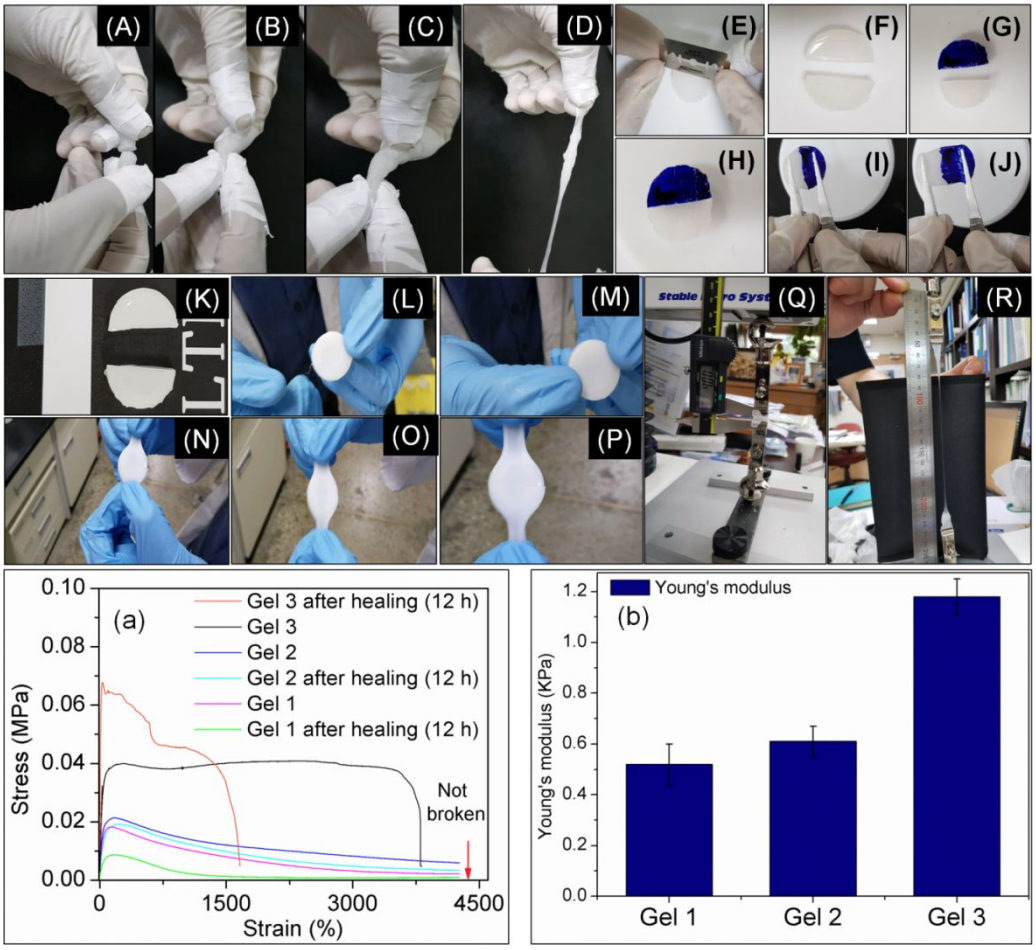

Figure 5. Healing test images of Gel 1(A-D), Gel 2 (E-J), Gel 3 (K-P), and pictures of tensile test set up (Q-R), tensile test results of three gels before and after 12 h of healing (a), and Young's modulus (b) of three Gels using TA.XT plus texture analyser.

The values of Young's modulus of three native gels were also determined from tensile experimentation (**Figure 5b**). Young's modulus values clearly increased as monomer concentrations increased, perhaps because of an increase in crosslinking density in the

hydrogel as monomer concentrations increase. Young's modulus values of Gel 1, Gel 2, and Gel 3 were measured as 0.52 ± 0.08, 0.61 ± 0.06, 1.18 ± 0.07 KPa, respectively (**Figure 5b).**

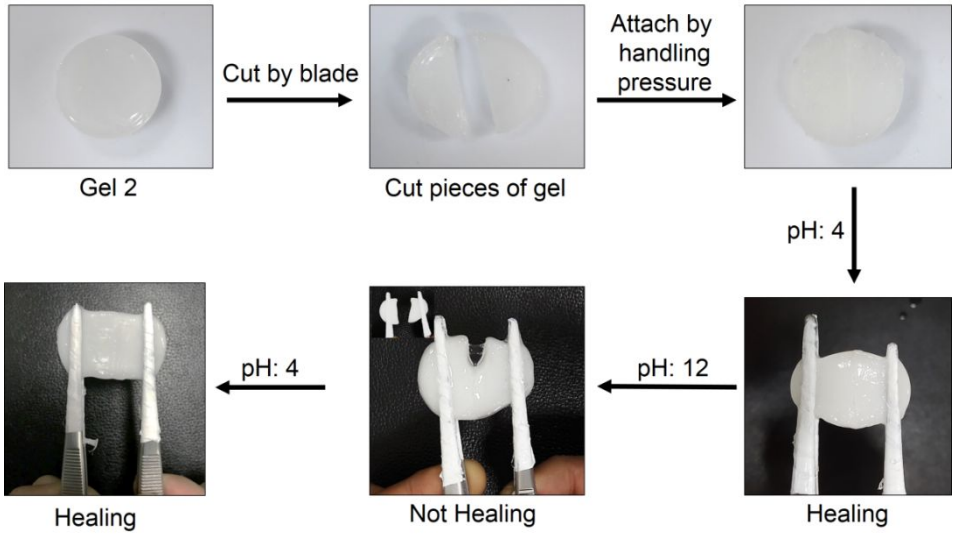

Figure 6. pH-responsive healing behaviour of PAA-PMMA gel (Gel 2)

Figure 6 summarizes the pH-responsive self-healing behaviour of the hydrogel. Results revealed that the formation of hydrogen bonds is reversible and depends on the pH of the solution. At pH 4.5, when cut species came in contact with one another, they attached through corresponding hydrogen bonds between $–OCH_3$ groups and carboxylic groups, and hence gain self-healing capacity. Meanwhile, at pH 12, the carboxylic acid groups in the hydrogel pieces deprotonated and formed carboxylate anions. Consequently, when two pieces come in contact, electrostatic repulsive force prevents healing and leads to separation **(Figure 6**). Again, when the separated hydrogels were re-entered into pH 4.5 medium, carboxylate ions protonated and formed carboxylic acid groups, thus reconstructing hydrogen bonding enabling for the recovery of healing capacity **(Figure 6**). The results suggest the pH-responsive reversibility of the self-healing capacity of the prepared gel and also confirmed that weak hydrogen bonds are predominantly responsible for the healing capacity.

3.4. Compression test results of the hydrogel

Figure 7 reveals the compression test results of three gels and the mineralized gels. The compression stress-strain plot (**Figure 7a** and **Table S5, Supporting Information**), reveals that Gel 3 had the highest compressive modulus value (0.147 ± 0.005 MPa) compared to Gel 2 (0.093 ± 0.002 MPa) and Gel 1 (0.070 ± 0.003 MPa) at 50 N force. The presence of the highest concentration of monomers in Gel 3 increased crosslinking density, thus resulting in the greatest compressive modulus value. It is also clear that the compressive modulus value of the gels decreased after mineralization, a characteristic that may be due to the rupture of the hydrogen bond-crosslinking network in the gel matrix during the medium change to pH 7.4. In this medium, deprotonation of the carboxylic acid groups occurred and a repulsive interaction was created among negatively charged carboxylate ions which distorted the orientation of the polymer chains in the network. The compressive modulus values of the mineralized Gel 1-M, Gel 2-M, and Gel 3-M were 0.032 ± 0.002, 0.047 ± 0.002, and 0.060 ± 0.003 MPa, respectively (**Figure 7a** and **Table S5, Supporting Information**), which signified ~22%, ~51% and ~85% decreases of modulus after mineralization of Gel 1, Gel 2 and Gel 3, respectively. These results indicate that higher AA-containing gels are associated with higher mineralization and lower Young's modulus values.

To identify the self-recoverability of the prepared gels, seven consecutive hysteresis tests were carried through loading−unloading processes at 70 % strain and 20 N force without any interval time between the cycles. As presented in **Figure 7b-d**, the hysteresis loop occurs in each cycle between the loading and unloading curves of each gel. The dissipation energy after each cycle was calculated by measuring the hysteresis area (**Figure 7e**). **Figure 7b-d** reveals that the self-recoverability of Gel 3 is better than Gel 2 and Gel 1.

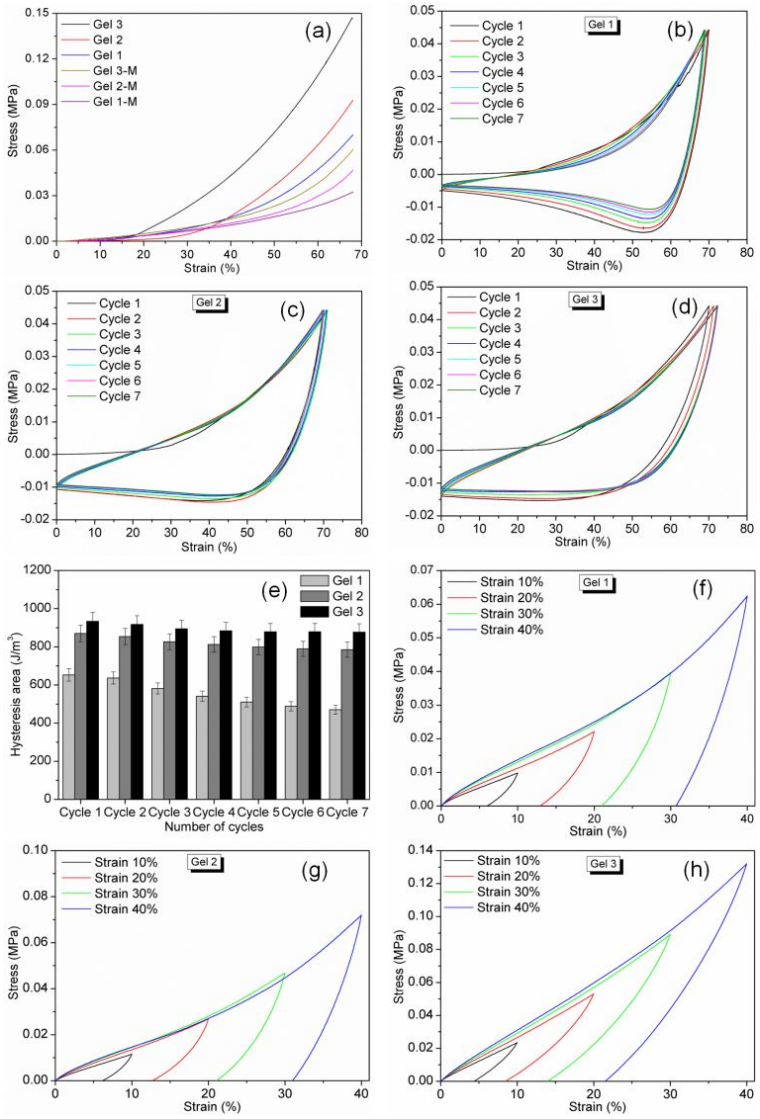

Figure 7. Compression test results: (a) Normal stress *vs*. strain (%) plot of native gel and mineralized gels, (b-d) cycle test of three gels, (e) hysteresis area of 7 cycles, and (f-h) strain variation results of three gels.

It is further observed that the energy of dissipation of Gel 3 decreased from 933.3 ± 46.6 J/m^3 to 876.8 ± 43.8 J/m3 from cycle 1 to cycle 7, compared with 869.8 ± 43.9 J/m^3 to 784.5 ± 39.2 J/m^3, and 652.5 ± 32.6 J/m^3 to 469.9 ± 23.4 J/m^3 for Gel 2 and Gel 1, respectively (**Figure 7e**). The dissipated energies recovered after the 7th cycle for Gel 1, Gel 2, and Gel 3 were ~72 %, ~90 %, and ~94 %, respectively. These results indicate better shape

recoverability of Gel 3 compared with Gel 1 and Gel 2. This improvement may be resulting from higher cross-linking density through hydrogen bonds, which work as reversible sacrificial cross-linker helping the gel retain its original shape. When strain variation (10 %, 20 %, 30 %, and 40 %) experiments were performed using 50 N force, all gels showed self-recoverability up to 30 % strain (**Figure 7f-h**) and the nature of the stress-strain plot of Gel 3 (**Figure 7 h**) demonstrates better self-recoverability than those of Gel 2 and Gel 1.

3.5. Adhesive test

Hydrogel adhesion is an important characteristic for biomedical and industrial applications. The adhesiveness of hydrogels is principally due to the presence of different functional groups (hydrophilic and/or hydrophobic) at the interface of the network. Generally, a hydrogel is adherent to the surface of a test material through either chemical or physical interaction (ionic, H-bonding or van der Waals force) between the functional groups present on the surfaces of both hydrogel and test material. Adhesion also depends on the composition of the gel network, chemical structure, conformation as well as orientation of side chains of the substrates. **Figure 8** reveals that Gel 2 is strongly adherent on the surfaces of polystyrene dish (**Figure 8a**), glass vial (**Figure 8b**), wood (**Figure 8c**), stainless steel rod (**Figure 8d**), ceramics ball (**Figure 8e**), stone (**Figure 8e**), iron (**Figure 8f**), human skin (**Figure 8g-j**) and pork skin (**Figure 8 k-l**). Furthermore, the developed gel can form layer-by-layer structures with pork skin (**Figure 8l**). When the concentration of MMA in the gel network was increased, adhesiveness decreased. This is maybe due to the presence of higher numbers of hydrophobic units and the formation of a rigid network where the flexibility of polymer chains is low. The amount of adhesive forces and adhesive energies of Gel 1, Gel 2, and Gel 3 on polystyrene dish, glass vial, wood, stainless steel rod, ceramics ball, stone, iron, and pork skin are reported in **Figure S8-S10** and **Table S6, Supporting Information**). In

contrast, the mineralized gels have not shown adhesiveness towards those objects.

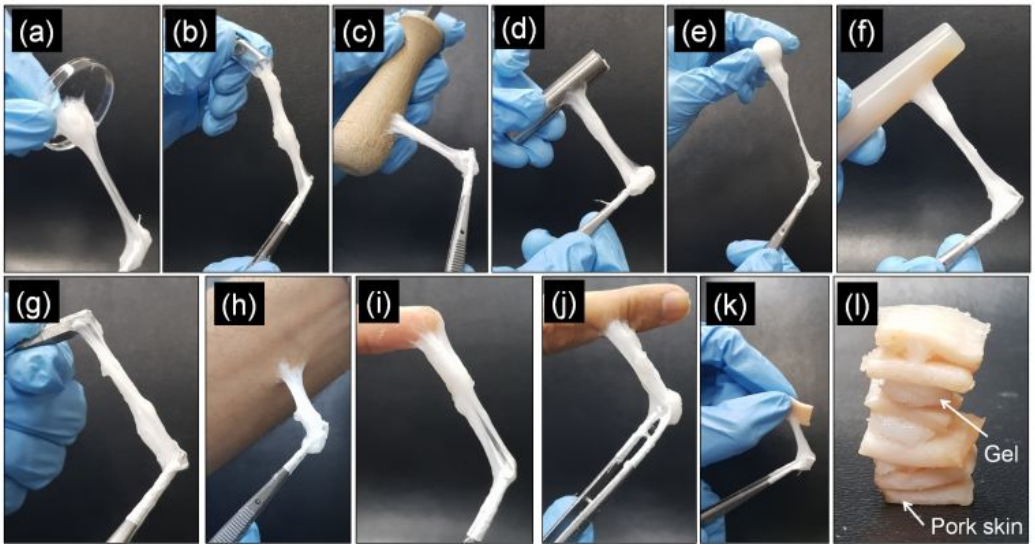

Figure 8. Digital images of the adhesiveness of Gel 2 on the surfaces of (a) polystyrene, (b) glass, (c) wood, (d) stainless steel, (e) ceramics, (f) stone, (g) iron, (h-j) human skin, (k) pork skin, (l) multilayers of pork skin.

3.6. Swelling study

Swelling study results indicate that the prepared hydrogel showed a pH-responsive swelling nature (**Figure 9**). All employed gels were associated with greater % swelling in basic medium (pH 7.4) compared with acidic medium (pH 4.5). At pH 7.4, deprotonation of carboxylic acid groups of the PAA-PMMA gels occurred, which increased the hydrophilicity of the polymer, and thus the polymers absorb more water molecules and increased swelling. Gel 3 displayed the lowest % swelling after 24 h. As the amount of MMA increased, the hydrophilicity of the polymers decreased and their crosslinking density increased, which results in % swelling order of Gel 1 > Gel 2 > Gel 3.

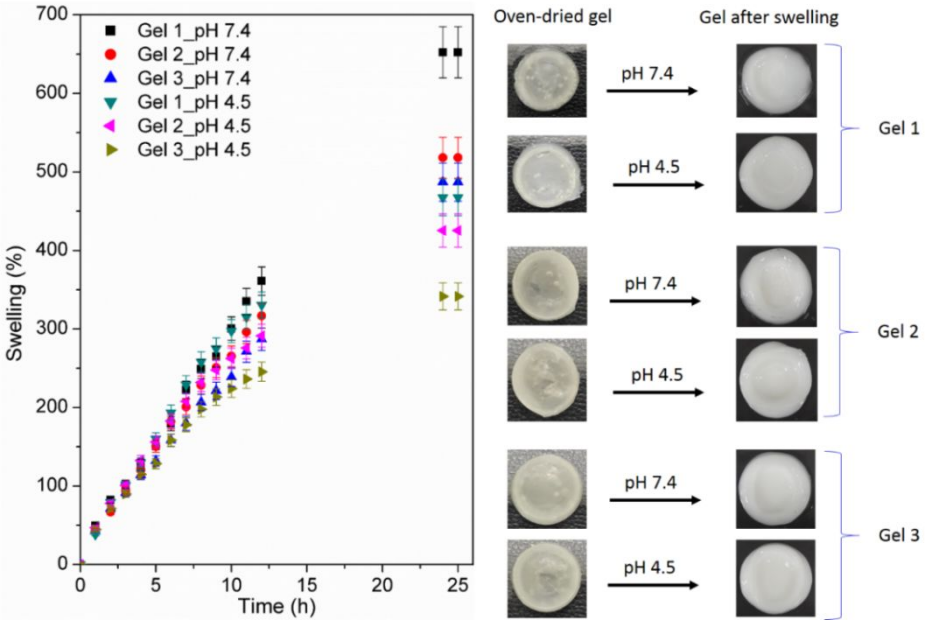

Figure 9. Swelling study results of three gels at pH 4.5/7.4 and 37 ± 0.5 °C

3.7. *In vitro* cell culture study and effect of mineralization of cell adhesion

An *in vitro* cell study was executed using the MC3T3 cell line (p=11). Cultured cells on the well plate were covered with the hydrogel and the effect of cell adhesion was quantified. It has been reported that a PAA-based hydrogel can serve as a template for calcium phosphate mineralization because of the presence of carboxylic acid groups which have a strong attraction toward calcium ions [3]. Similarly, here the developed hydrogel was used as a template for mineralization of calcium phosphate (**Figure S11, Supporting Information**). The changed topography of hydrogel (detected by HR-FESEM) confirmed that excellent microstructures formed by calcium phosphate mineralization on the surface of the hydrogel (**Figure 4d-f**). It has been reported that the micro- or nano-structures of calcium phosphate play a crucial function in regulating cell behaviour[3]. From the optical density values (**Figure 10a**), it is obvious that on day 1, the growth rate of the MC3T3 cell on the control (well plate) was higher than those samples treated with hydrogels. However, on days 3 and 5, cells have

grown significantly in the presence of mineralized gels, even higher than those of native Gel 2 and the control. On day 5, the number of live cells decreased only in the presence of Gel 2 which indicates the toxic nature of Gel 2 (**Figure 10A** and **10b**).

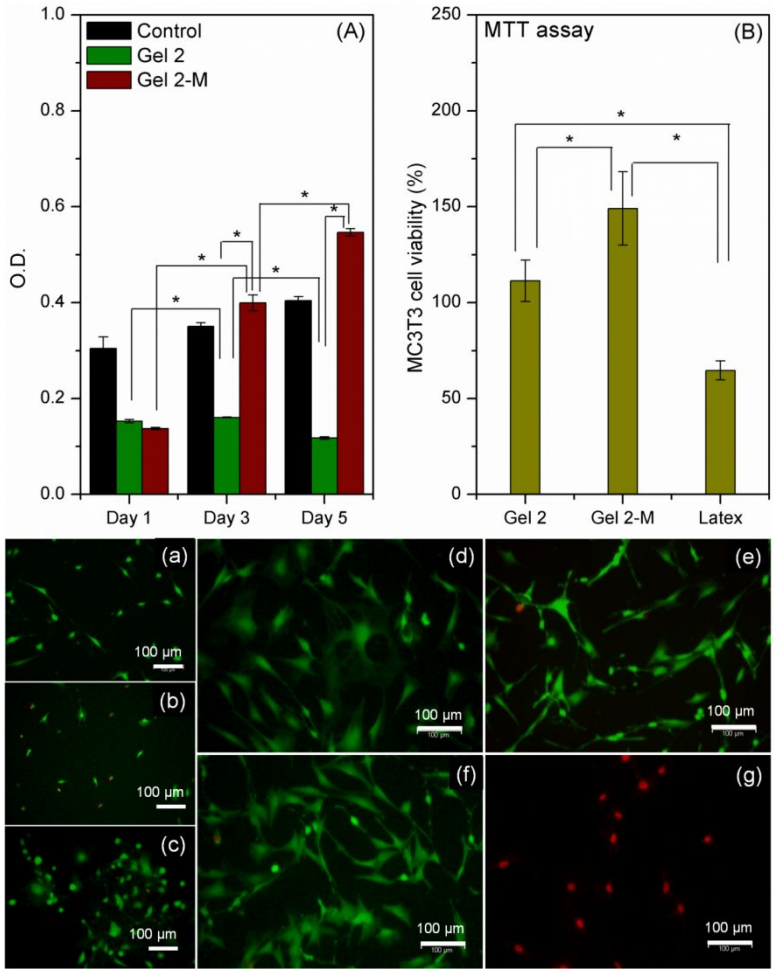

Figure 10. (A) Optical density of cultured MC3T3 cell on well plate (control), covered by Gel 2, mineralized Gel 2 (Gel 2-M) and (a-c) their corresponding live and dead cell images after 5 days, respectively, (B) MC3T3 cell viability results, and their corresponding live and dead cell images after 1 day in presence extracts of Teflon (considered as 100 %) (d), Gel 2(e), Gel 2-M(f), latex(g).

In Gel 2-M, carboxylate ions are ionically crosslinked with calcium ions prevent the pH of the medium from changing. The significant increases of the optical density in the presence

of mineralized Gel 2 (Gel 2-M) signifies that calcium phosphate mineralisation creates a biologically active surface and hence increased cell viability and functionality[3]. The live and dead cell images after day 5 also support improved cell adhesiveness of Gel 2-M (**Figure 10a-c**). On the other hand, the mineralized gel revealed no adhesiveness towards different objects owing to the existence of calcium phosphate particles on the surface of the hydrogels. The results of the cell viability studies of the swelled native Gel 2, Gel 2-M (at pH 7.4) suggested that native Gel-2 has shown toxicity after 5 days, however, mineralized Gel-2 is biocompatible and non-toxic to MC3T3 cells.

4. Conclusions

Weak hydrogen bond and hydrophobic interaction creating highly stretchable, self-healing and adhesive polymeric hydrogel (PAA-PMMA), was successfully synthesized by controlling the compositions of two immiscible monomers (ie, MMA and AA) *via* aqueous free radical polymerization. Experimental results signified that at a specific molar ratio of MMA and AA, the synthesized gel becomes self-healable, a trait attributed to the formation of hydrophobic interaction between methyl groups ($-CH_3$) of PMMA domain as well as weak hydrogen-bonding interaction between the –COOH groups of PAA and methoxy groups ($-OCH_3$) of PMMA units. Both hydrogen bonding and hydrophobic interaction rupture and reform, giving the PAA-PMMA hydrogels effectual energy dissipation capacity and self-recoverability. The prepared gels had different degrees of reversible healing depending on the pHs and molar ratio of AA and MMA. The hydrogel is adhesive on the surfaces of varying materials (eg, polystyrene dish, glass vial, wood, stainless steel rod, ceramics ball, stone, iron, human skin, and pork skin). Additionally, the gel can act as a template for calcium phosphate mineralization to fabricate a hydrogel composite which improved cell adhesion and proliferation. Finally, it is envisioned that the hydrogel synthesized from MMA and AA using

a simple method and having highly desirable characteristics, may have applications in industrial and biomedical industries.

<Supporting Information>

Synthesis details of hydrogel (Table S1); details of *in vitro* cell study and cytotoxicity study; DSC and TGA plots (Figure S1); EDAX results (Figure S2-S4, Table S2-S4); digital images of hydrogels after tensile test (Figure S5); tensile results of healed gels after 1 h (Figure S6); possible interactions in gel system (Figure S7); values of compressive modulus (Table S5); data regarding adhesive forces and adhesive energies (Figure S8-S10, Table S6); digital images of gels before and after mineralization (Figure S11).

Acknowledgements

The authors are grateful to the financial support of the National Research Foundation of Korea (NRF) Grant (2015R1A2A1A10054592). Recently, Dr. Dipankar Das is doing Postdoctoral research under Alexander von Humboldt fellowship in the Department of Physical Chemistry I and Research Center of Micro and Nano-chemistry and Engineering (Cμ), University of Siegen, Germany. We are also thankful to Mr. Cheol Kang for his assistance during texture analysis.

Authors contributions

Dr. Dipankar Das designed and performed most of the experiments, and wrote the manuscript. Ms. Euncheong Cha and Ms. Sangji Lee conducted cell-study experiments, and Mr. HyunSoo Shin conducted the swelling and mineralization study. Prof. Insup Noh supervised the research.

Conflicts of Interest

There are no conflicts of interest to declare.

References

1. Tong, X.; Du, L.; Xu, Q., Tough, adhesive and self-healing conductive 3D network hydrogel of physically linked functionalized-boron nitride/clay /poly(N-isopropylacrylamide). *J. Mater. Chem. A* **2018,** 6, (7), 3091-3099.
2. Lei, Z.; Wang, Q.; Sun, S.; Zhu, W.; Wu, P., A Bioinspired Mineral Hydrogel as a Self-Healable, Mechanically Adaptable Ionic Skin for Highly Sensitive Pressure Sensing. *Adv. Mater.* **2017,** 29, (22).
3. Teng, L.; Chen, Y.; Jin, M.; Jia, Y.; Wang, Y.; Ren, L., Weak Hydrogen Bonds Lead to Self-Healable and Bioadhesive Hybrid Polymeric Hydrogels with Mineralization-Active Functions. *Biomacromolecules* **2018,** 19, (6), 1939-1949.
4. Chen, Q.; Zhu, L.; Chen, H.; Yan, H. L.; Huang, L. N.; Yang, J.; Zheng, J., A Novel Design Strategy for Fully Physically Linked Double Network Hydrogels with Tough, Fatigue Resistant, and Self-Healing Properties. *Adv. Funct. Mater.* **2015,** 25, (10), 1598-1607.
5. Neal, J. A.; Mozhdehi, D.; Guan, Z., Enhancing Mechanical Performance of a Covalent Self-Healing Material by Sacrificial Noncovalent Bonds. *J. Am. Chem. Soc.* **2015,** 137, (14), 4846-4850.
6. Halacheva, S. S.; Adlam, D. J.; Hendow, E. K.; Freemont, T. J.; Hoyland, J.; Saunders, B. R., Injectable Biocompatible and Biodegradable pH-Responsive Hollow Particle Gels Containing Poly(acrylic acid): The Effect of Copolymer Composition on Gel Properties. *Biomacromolecules* **2014,** 15, (5), 1814-1827.
7. Getachew, B. A.; Kim, S.-R.; Kim, J.-H., Self-Healing Hydrogel Pore-Filled Water Filtration Membranes. *Environ. Sci. Technol.* **2017,** 51, (2), 905-913.
8. Li, J.; Geng, L.; Wang, G.; Chu, H.; Wei, H., Self-Healable Gels for Use in Wearable Devices. *Chem. Mater.* **2017,** 29, (21), 8932-8952.
9. Hou, J.; Liu, M.; Zhang, H.; Song, Y.; Jiang, X.; Yu, A.; Jiang, L.; Su, B., Healable green hydrogen bonded networks for circuit repair, wearable sensor and flexible electronic devices. *J. Mater. Chem. A* **2017,** 5, (25), 13138-13144.
10. Deng, Z.; Guo, Y.; Zhao, X.; Ma, P. X.; Guo, B., Multifunctional Stimuli-Responsive Hydrogels with Self-Healing, High Conductivity, and Rapid Recovery through Host–Guest Interactions. *Chem. Mater.* **2018,** 30, (5), 1729-1742.
11. Wang, Y.; Huang, F.; Chen, X.; Wang, X.-W.; Zhang, W.-B.; Peng, J.; Li, J.; Zhai, M., Stretchable, Conductive, and Self-Healing Hydrogel with Super Metal Adhesion. *Chem. Mater.* **2018,** 30, (13), 4289-4297.
12. Liu, Y.-J.; Cao, W.-T.; Ma, M.-G.; Wan, P., Ultrasensitive Wearable Soft Strain Sensors of Conductive, Self-healing, and Elastic Hydrogels with Synergistic "Soft and Hard" Hybrid Networks. *ACS Appl. Mater. Interfaces* **2017,** 9, (30), 25559-25570.
13. Jing, X.; Mi, H.-Y.; Peng, X.-F.; Turng, L.-S., Biocompatible, self-healing, highly stretchable polyacrylic acid/reduced graphene oxide nanocomposite hydrogel sensors via mussel-inspired chemistry. *Carbon* **2018,** 136, 63-72.
14. Liu, X.; Zhang, Q.; Gao, Z.; Hou, R.; Gao, G., Bioinspired Adhesive Hydrogel Driven by Adenine and Thymine. *ACS Appl. Mater. Interfaces* **2017,** 9, (20), 17645-17652.
15. Chen, Y.; Diaz-Dussan, D.; Wu, D.; Wang, W.; Peng, Y.-Y.; Asha, A. B.; Hall, D. G.; Ishihara, K.; Narain, R., Bioinspired Self-Healing Hydrogel Based on Benzoxaborole-Catechol Dynamic Covalent Chemistry for 3D Cell Encapsulation. *ACS Macro Lett.* **2018,** 7, (8), 904-908.
16. Wang, X.-H.; Song, F.; Qian, D.; He, Y.-D.; Nie, W.-C.; Wang, X.-L.; Wang, Y.-Z., Strong and tough fully physically crosslinked double network hydrogels with tunable mechanics and high self-healing performance. *Chem. Eng. J.* **2018,** 349, 588-594.
17. Chen, N.; Qin, L.; Pan, Q., Mussel-inspired healing of a strong and stiff polymer. *J. Mater. Chem. A* **2018,** 6, (15), 6667-6674.
18. Palleau, E.; Reece, S.; Desai, S. C.; Smith, M. E.; Dickey, M. D., Self-Healing Stretchable Wires for Reconfigurable Circuit Wiring and 3D Microfluidics. *Adv. Mater.* **2013,** 25, (11), 1589-1592.
19. Thakur, V. K.; Kessler, M. R., Self-healing polymer nanocomposite materials: A review. *Polymer* **2015,** 69, 369-383.

20. Heo, Y.; Sodano, H. A., Self-Healing Polyurethanes with Shape Recovery. *Adv. Funct. Mater.* **2014,** 24, (33), 5261-5268.
21. Oehlenschlaeger, K. K.; Mueller, J. O.; Brandt, J.; Hilf, S.; Lederer, A.; Wilhelm, M.; Graf, R.; Coote, M. L.; Schmidt, F. G.; Barner-Kowollik, C., Adaptable Hetero Diels–Alder Networks for Fast Self-Healing under Mild Conditions. *Adv. Mater.* **2014,** 26, (21), 3561-3566.
22. Froimowicz, P.; Frey, H.; Landfester, K., Towards the Generation of Self-Healing Materials by Means of a Reversible Photo-induced Approach. *Macromol. Rapid Commun.* **2011,** 32, (5), 468-473.
23. Xu, W. M.; Rong, M. Z.; Zhang, M. Q., Sunlight driven self-healing, reshaping and recycling of a robust, transparent and yellowing-resistant polymer. *J. Mater. Chem. A* **2016,** 4, (27), 10683-10690.
24. Ghosh, B.; Urban, M. W., Self-Repairing Oxetane-Substituted Chitosan Polyurethane Networks. *Science* **2009,** 323, (5920), 1458-1460.
25. Hu, X.; Vatankhah-Varnoosfaderani, M.; Zhou, J.; Li, Q.; Sheiko, S. S., Weak Hydrogen Bonding Enables Hard, Strong, Tough, and Elastic Hydrogels. *Adv. Mater.* **2015,** 27, (43), 6899-6905.
26. Hörning, M.; Nakahata, M.; Linke, P.; Yamamoto, A.; Veschgini, M.; Kaufmann, S.; Takashima, Y.; Harada, A.; Tanaka, M., Dynamic Mechano-Regulation of Myoblast Cells on Supramolecular Hydrogels Cross-Linked by Reversible Host-Guest Interactions. *Sci. Rep.* **2017,** 7, (1), 7660.
27. Dankers, P. Y. W.; Hermans, T. M.; Baughman, T. W.; Kamikawa, Y.; Kieltyka, R. E.; Bastings, M. M. C.; Janssen, H. M.; Sommerdijk, N. A. J. M.; Larsen, A.; van Luyn, M. J. A.; Bosman, A. W.; Popa, E. R.; Fytas, G.; Meijer, E. W., Hierarchical Formation of Supramolecular Transient Networks in Water: A Modular Injectable Delivery System. *Adv. Mater.* **2012,** 24, (20), 2703-2709.
28. Jeon, I.; Cui, J.; Illeperuma, W. R. K.; Aizenberg, J.; Vlassak, J. J., Extremely Stretchable and Fast Self-Healing Hydrogels. *Adv. Mater.* **2016,** 28, (23), 4678-4683.
29. Hu, X.; Zhou, J.; Vatankhah-Varnosfaderani, M.; Daniel, W. F. M.; Li, Q.; Zhushma, A. P.; Dobrynin, A. V.; Sheiko, S. S., Programming temporal shapeshifting. *Nat. Commun.* **2016,** 7, 12919.
30. Phadke, A.; Zhang, C.; Arman, B.; Hsu, C.-C.; Mashelkar, R. A.; Lele, A. K.; Tauber, M. J.; Arya, G.; Varghese, S., Rapid self-healing hydrogels. *Proc. Natl. Acad. Sci. U. S. A.* **2012,** 109, (12), 4383-4388.
31. Shih, C.-C.; Wu, K.-H.; Chang, T.-C.; Liu, H.-K., Characterization, chain mobility, and thermal properties of the hydrophilic poly(methyl methacrylate-co-acrylic acid) colloids. *Polym. Compos.* **2008,** 29, (1), 37-44.
32. Oliveira, M. A. S.; Moraes, J. J.; Faez, R., Impedance studies of poly(methylmethacrylate-co-acrylic acid) doped polyaniline films on aluminum alloy. *Prog. Org. Coat.***2009,** 65, (3), 348-356.
33. Sayar, F.; Güven, G.; Pişkin, E., Magnetically loaded poly(methyl methacrylate-co-acrylic acid) nano-particles. *Colloid Polym. Sci.* **2005,** 284, (9), 965.
34. Barba, A. A.; Dalmoro, A.; De Santis, F.; Lamberti, G., Synthesis and characterization of P(MMA-AA) copolymers for targeted oral drug delivery. *Polym. Bull.* **2009,** 62, (5), 679-688.
35. Gyurova, A. Y.; Halacheva, S.; Mileva, E., Aqueous solutions of random poly(methyl methacrylate-co-acrylic acid): effect of the acrylic acid content. *RSC Adv.* **2017,** 7, (22), 13372-13382.
36. Yan, X.; Gemeinhart, R. A., Cisplatin delivery from poly(acrylic acid-co-methyl methacrylate) microparticles. *J. Controlled Release* **2005,** 106, (1), 198-208.
37. Ekpenyong, K. I., Monomer reactivity ratios: Acrylic acid-methylmethacrylate copolymerization in dimethylsulfoxide. *J. Chem. Educ.* **1985,** 62, (2), 173.
38. Das, D.; Zhang, S.; Noh, I., Synthesis and characterizations of alginate-α-tricalcium phosphate microparticle hybrid film with flexibility and high mechanical property as a biomaterial. *Biomed. Mater.* **2018,** 13, (2), 025008.
39. Das, D.; Pham, T. T. H.; Noh, I., Characterizations of hyaluronate-based terpolymeric hydrogel synthesized via free radical polymerization mechanism for biomedical applications. *Colloids Surf., B* **2018,** 170, 64-75.
40. Das, D.; Ghosh, P.; Ghosh, A.; Haldar, C.; Dhara, S.; Panda, A. B.; Pal, S., Stimulus-Responsive, Biodegradable, Biocompatible, Covalently Cross-Linked Hydrogel Based on Dextrin and Poly(N-isopropylacrylamide) for in Vitro/in Vivo Controlled Drug Release. *ACS Appl. Mater. Interfaces* **2015,** 7, (26), 14338-14351.

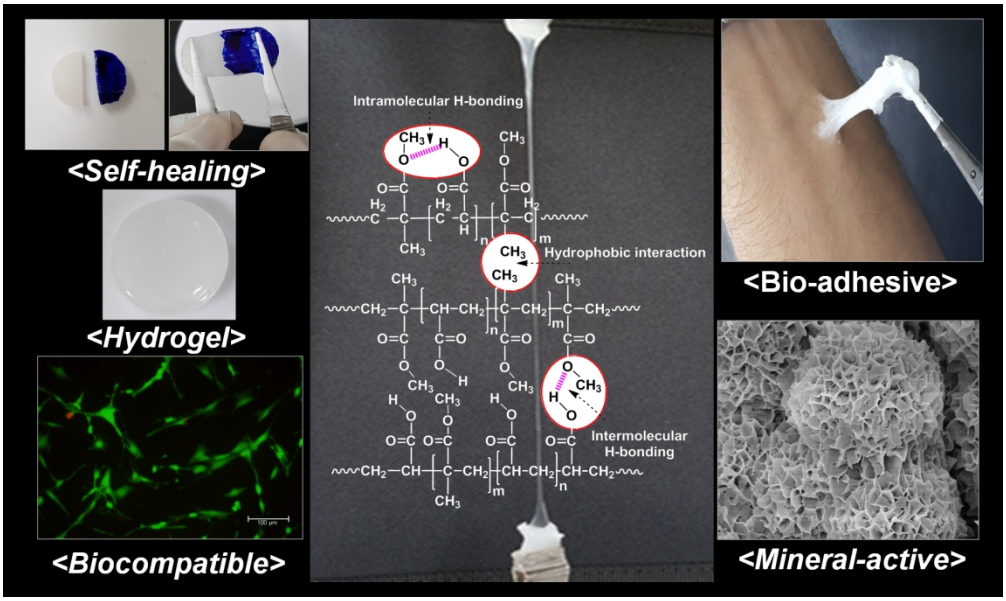

534x316mm (96 x 96 DPI)